nature structural & molecular biology

The pilus usher controls protein interactions via domain masking and is functional as an oligomer

Glenn T Werneburg[1,2], Nadine S Henderson[1,2], Erica B Portnoy[1,2], Samema Sarowar[3,4], Scott J Hultgren[5,6], Huilin Li[3,4] & David G Thanassi[1,2]

The chaperone-usher (CU) pathway assembles organelles termed pili or fimbriae in Gram-negative bacteria. Type 1 pili expressed by uropathogenic *Escherichia coli* are prototypical structures assembled by the CU pathway. Biogenesis of pili by the CU pathway requires a periplasmic chaperone and an outer-membrane protein termed the usher (FimD). We show that the FimD C-terminal domains provide the high-affinity substrate-binding site but that these domains are masked in the resting usher. Domain masking requires the FimD plug domain, which serves as a switch controlling usher activation. We demonstrate that usher molecules can act in *trans* for pilus biogenesis, providing conclusive evidence for a functional usher oligomer. These results reveal mechanisms by which molecular machines such as the usher regulate and harness protein-protein interactions and suggest that ushers may interact in a cooperative manner during pilus assembly in bacteria.

The CU pathway is a conserved secretion system dedicated to the assembly of virulence-associated organelles termed pili or fimbriae in Gram-negative bacteria[1–4]. The type 1 and P pili expressed by uropathogenic *E. coli* are prototypical structures assembled by the CU pathway[5,6]. CU pili are linear polymers composed of multiple different subunit proteins (pilins). The assembled pilus adopts a composite architecture consisting of a rigid helical rod that is anchored to the outer membrane (OM) and a flexible tip fiber that contains the adhesive subunit (adhesin). The type 1–pilus rod contains more than 1,000 copies of the FimA major pilin; the type 1–pilus tip contains the FimH adhesin at its distal end, which is followed by single copies of the FimG and FimF adaptor subunits[7,8] (**Fig. 1a**). FimH binds to mannosylated proteins present on the bladder epithelium, and this can lead to bacterial invasion and the development of cystitis[5].

The CU pathway assembles and secretes pili in a highly regulated manner (**Fig. 1a**). Nascent pilins enter the periplasm via the Sec translocon[9] and then form binary complexes with the periplasmic chaperone in a process termed donor-strand complementation (DSC)[10,11]. In DSC, the chaperone donates a β-strand to complete the incomplete immunoglobulin-like fold of the subunit[10–12] (structure shown in **Supplementary Fig. 1a**). For assembly of subunits into a pilus fiber and secretion to the cell surface, chaperone–subunit complexes must interact with the OM usher. The usher catalyzes the exchange of chaperone-subunit for subunit-subunit interactions[13]. Subunit-subunit interactions form by a mechanism termed donor-strand exchange (DSE)[12,14], in which the N-terminal extension of an incoming subunit replaces the donated chaperone β-strand from the preceding subunit (**Supplementary Fig. 1b**). Type 1 pili are assembled starting with the FimH adhesin, and the pilus extends by stepwise addition of new chaperone–subunit complexes to the base of the fiber (**Fig. 1a**). Each subunit specifically interacts with its appropriate neighbor in the pilus, with the specificity of binding determined by the DSE reaction[15,16]. In addition, the usher aids in ordered pilus assembly by differentially recognizing chaperone–subunit complexes[16–19].

Ushers are large integral OM proteins composed of five domains[20–23]: a periplasmic N-terminal (N) domain, a transmembrane β-barrel channel domain, a plug domain located within the β-barrel region and two periplasmic C-terminal domains (C1 and C2) (**Fig. 1** and **Supplementary Fig. 1**). The N domain provides the initial binding site for chaperone–subunit complexes[21,24–26] (schematic and structure shown in **Figs. 1a** and **2a**, respectively). The C1 and C2 domains provide a second binding site and anchor the growing pilus fiber[23,27,28] (schematic and structure shown in **Figs. 1a** and **2b**, respectively). In the resting apo-FimD usher, the plug domain occludes the lumen of the β-barrel channel[20,22,23] (structure shown in **Supplementary Fig. 1c**). The usher must be activated for pilus biogenesis by binding of a FimC–FimH complex to the N domain[13,18,29]. Activation results in displacement of the plug to the periplasm, insertion of the FimH adhesin into the channel lumen and transfer of FimC–FimH from the usher N domain to the C domains[23] (structure shown in **Fig. 2b**). The mechanism and specific sequence of events driving usher activation and handoff of chaperone–subunit complexes from the N to the C domains is not understood. The usher N and C domains

[1]Center for Infectious Diseases, Stony Brook University, Stony Brook, New York, USA. [2]Department of Molecular Genetics and Microbiology, Stony Brook University, Stony Brook, New York, USA. [3]Department of Biochemistry and Cell Biology, Stony Brook University, Stony Brook, New York, USA. [4]Biosciences Department, Brookhaven National Laboratory, Upton, New York, USA. [5]Department of Molecular Microbiology, Washington University School of Medicine, Saint Louis, Missouri, USA. [6]Center for Women's Infectious Disease Research, Washington University School of Medicine, Saint Louis, Missouri, USA. Correspondence should be addressed to D.G.T. (david.thanassi@stonybrook.edu).

Received 5 November 2014; accepted 12 May 2015; published online 8 June 2015; doi:10.1038/nsmb.3044

bind to the same surface of the chaperone, and handoff requires rotation of the chaperone–subunit complex, concomitant with translocation of the pilus fiber through the usher channel toward the cell surface[21,23,26,27]. The usher exists in the OM as an oligomer[20,28,30,31]. However, the pilus fiber is secreted through only one protomer of the usher oligomer, and the usher monomer appears to be sufficient for pilus biogenesis[20,23,27,32]. Therefore, whether and how the additional usher molecules contribute to the catalysis of pilus assembly *in vivo* has been a subject of debate.

In this study, we sought to understand how the usher controls and coordinates protein-protein interactions during pilus biogenesis. We used site-directed photo-cross-linking to confirm the usher N, C1 and C2 domains as specific binding sites during pilus assembly *in vivo*. Using a fluorescence-based affinity assay to compare binding of FimC–FimH to wild-type (WT) and domain-deleted FimD ushers (**Fig. 1b**), we show that the FimD C domains provide the high-affinity binding site, thus suggesting that handoff of chaperone–subunit complexes from the N to the C domains is driven by differential affinity. We provide evidence that the C domains are masked in apo-FimD through interaction with the plug domain, thus explaining why FimC–FimH must first bind to the N domain to activate the usher. We also show that the plug domain is essential for fiber polymerization and acts as a switch controlling usher activation. Finally, by using a plug-deletion mutant to preactivate the usher, we demonstrate that the usher is functional as an oligomer *in vivo*.

RESULTS

FimD N and C domains are *in vivo* binding sites for FimC–FimH

We used site-directed photo-cross-linking via unnatural amino acid mutagenesis to map points of contact between chaperone–subunit complexes and the usher (**Fig. 2a**,**b**), as predicted by crystal structures of FimC–FimH bound to the FimD N domain or the complete FimD usher[21,23]. We constructed amber stop-codon (TAG) substitutions for residues in the N, C1 and C2 domains of FimD. We then transformed each FimD amber mutant together with a FimC–FimH expression plasmid into an *E. coli* strain containing plasmid pEVOL-pBpF, to allow incorporation of the photoreactive phenylalanine derivative *p*-benzoyl-phenylalanine (*p*Bpa) at the position of the amber stop codon[33]. We exposed bacteria grown in the presence of *p*Bpa to UV light to promote reaction of the carbonyl oxygen of *p*Bpa with nearby carbon-hydrogen bonds, to form stable cross-links[33,34].

We constructed and analyzed nine different FimD amber mutants, obtaining cross-links between the usher and the FimC chaperone or FimH adhesin for each mutant except one (**Supplementary Fig. 2a**). Each of these FimD amber mutants formed a stable usher in the OM in the presence of *p*Bpa, and each was functional for pilus assembly (data not shown). We obtained the most efficient cross-linking when *p*Bpa was located at FimD positions Phe4 in the N domain, Tyr704 and Thr717 in the C1 domain and Tyr788 in the C2 domain (**Fig. 2** and **Supplementary Figs. 2** and **3**). Cross-linked products that reacted with anti–FimC–FimH antibody were visible for each of these FimD amber mutants (**Fig. 2c**). The anti–FimC–FimH antibody cross-reacts with the histidine-tag epitope and thus also detects the histidine-tagged FimD usher. Immunoblotting with anti–histidine-tag antibody verified the presence of the usher in the cross-linked products, and analysis of a strain expressing a streptavidin-tagged FimD (which does not cross-react with the anti–FimC–FimH antibody) confirmed the presence of the chaperone or adhesin (**Supplementary Fig. 2b**,**c**). In addition, the cross-linked bands for the FimD Phe4, Thr717 and Tyr788 mutants, but not the Tyr704 mutant, reacted with anti–FimC–FimG antibody, which recognizes the FimC chaperone but not the FimH adhesin (**Fig. 2c**). When taken together, these results confirm the predicted interactions of FimD residues Phe4, Thr717 and Tyr788 with FimC, and FimD residue Tyr704 with FimH. More broadly, these results validate the N, C1 and C2 domains of the usher as specific binding sites for chaperone–subunit complexes during pilus biogenesis *in vivo*.

The bands obtained for the FimD Phe4 and Tyr788 amber mutants migrated at the expected size for a cross-linked FimD–FimC product (114 kDa; 91 kDa and 23 kDa for mature FimD and FimC, respectively) (**Fig. 2c**). We obtained a doublet for the FimD Phe4 mutant, with the lower band reacting with both the anti–FimC–FimH and

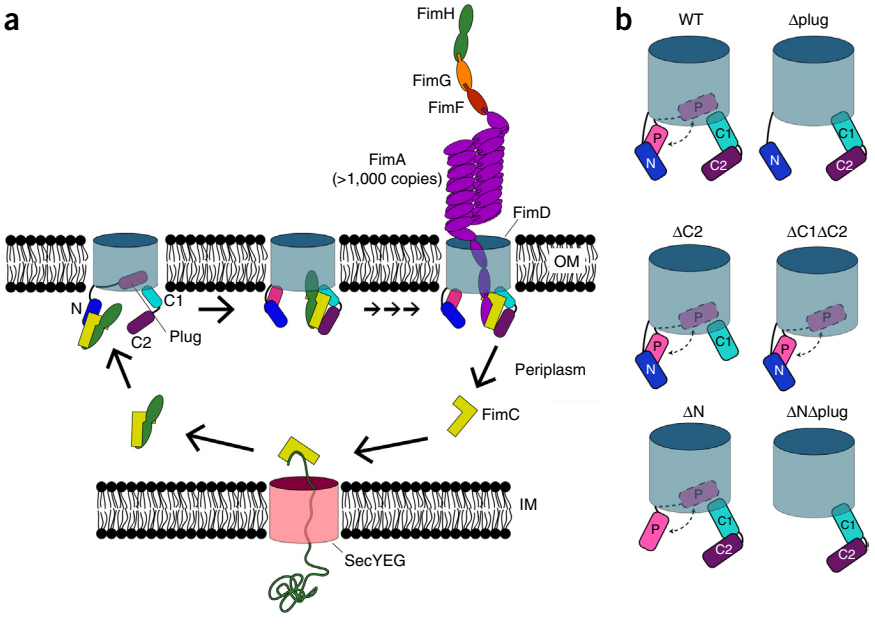

Figure 1 Models for type 1–pilus biogenesis and usher domain architecture. (**a**) Assembly of type 1 pili by the CU pathway. Pilus subunits traverse the inner membrane (IM) via the Sec translocon. Upon entering the periplasm, the subunits form binary complexes with the FimC chaperone (yellow). The chaperone enables proper folding of pilus subunits via the DSC mechanism (structural details in **Supplementary Fig. 1a**). Chaperone–subunit complexes next interact with the FimD usher. The usher is depicted as a monomer, with its β-barrel channel domain in the OM and its N, plug, C1 and C2 domains indicated. Binding of a chaperone–adhesin complex (FimC–FimH) to the N domain activates the usher for pilus biogenesis. The plug is expelled from the usher channel to accommodate the FimH adhesin, and the FimC–FimH complex is handed off from the N to the C domains. The N domain is then free to recruit additional chaperone–subunit complexes, which undergo DSE with the last-incorporated subunit bound at the C domains (structural details in **Supplementary Fig. 1b**). Repeated rounds of subunit recruitment and DSE result in assembly of the pilus fiber in a top-down manner and secretion through the usher channel to the bacterial surface. (**b**) Cartoon representations of WT FimD and the FimD domain-deletion mutants used in this study. The N, plug (P), C1 and C2 domains are indicated.

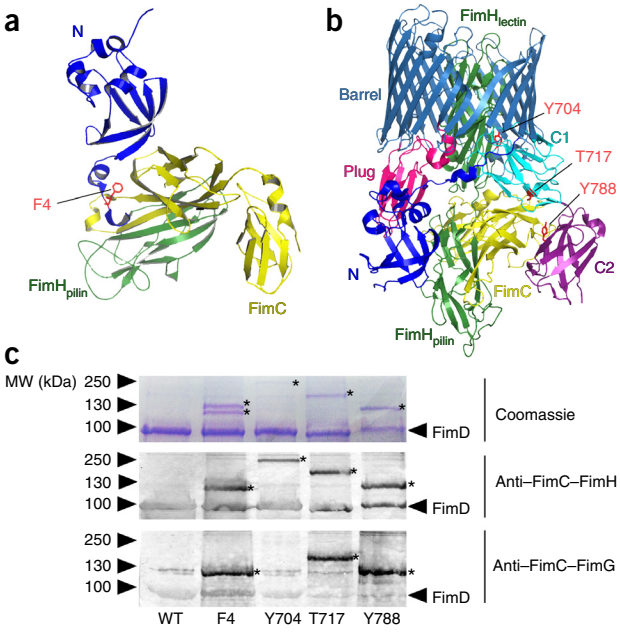

Figure 2 *In vivo* detection of FimC–FimH binding to the FimD usher. (**a**) Structure of the FimD N domain (blue) bound to a FimC–FimH pilin-domain (FimH$_{pilin}$) complex (yellow and green, respectively) (PDB 1ZE3 (ref. 21)). FimD residue Phe4 is depicted in red in stick representation. Phe4 is in proximity to the FimC chaperone (additional data in **Supplementary Fig. 2a**). (**b**) Structure of the FimD–FimC–FimH complex (PDB 3RFZ[23]). FimH is in green, FimC is in yellow, and the FimD domains are colored as in **Figure 1**. Residues Tyr704 (C1), Thr717 (C1) and Tyr788 (C2) are depicted in red in stick representation. Tyr704 is in proximity to the FimH adhesin domain (FimH$_{lectin}$), whereas Thr717 and Tyr788 are in proximity to the chaperone (additional data in **Supplementary Fig. 2b**). (**c**) SDS-PAGE and immunoblot analysis of *in vivo* site-directed photo-cross-linking. Samples are purified histidine-tagged WT FimD or FimD Phe4 (N domain), Tyr704 (C1 domain), Thr717 (C1 domain) or Tyr788 (C2 domain) amber mutants and associated cross-linked products. Additional controls are shown in **Supplementary Figure 2**. The position of the FimD monomer is indicated at right for each panel. The asterisks mark FimD-cross-linked products. Uncropped images are shown in **Supplementary Data Set 2**. MW, molecular weight.

anti–FimC–FimG antibodies, thus identifying it as the usher–chaperone complex (**Fig. 2c**). Mass spectrometry analysis confirmed the presence of FimD and FimC in the lower FimD Phe4 band as well as in the FimD Tyr788 cross-linked band (**Supplementary Data Set 1**). Mass spectrometry analysis of the upper band of the FimD Phe4 doublet suggested that this was a cross-link with the abundant OM protein OmpA (**Supplementary Data Set 1**). This is consistent with the usher having a dynamic and flexible N domain that is able to sample the periplasm for chaperone–subunit complexes. An *ompA*-mutant strain assembled type 1 pili similarly to the parental WT strain, as determined by hemagglutination (HA) assay (data not shown), a result indicating that that OmpA does not have a direct role in pilus biogenesis. In contrast to the FimD Phe4 and Tyr788 cross-linked products, the bands obtained for the FimD Tyr704 and Thr717 mutants migrated with slower relative mobility than expected for either a FimD–FimH complex (120 kDa, in comparison to 29 kDa for mature FimH) or a FimD–FimC complex, respectively (**Fig. 2c**). Mass spectrometry confirmed the presence of FimH and FimC in the cross-linked bands and did not identify other cross-linked partners for the FimD Tyr704 and Thr717 mutants (**Supplementary Data Set 1**).

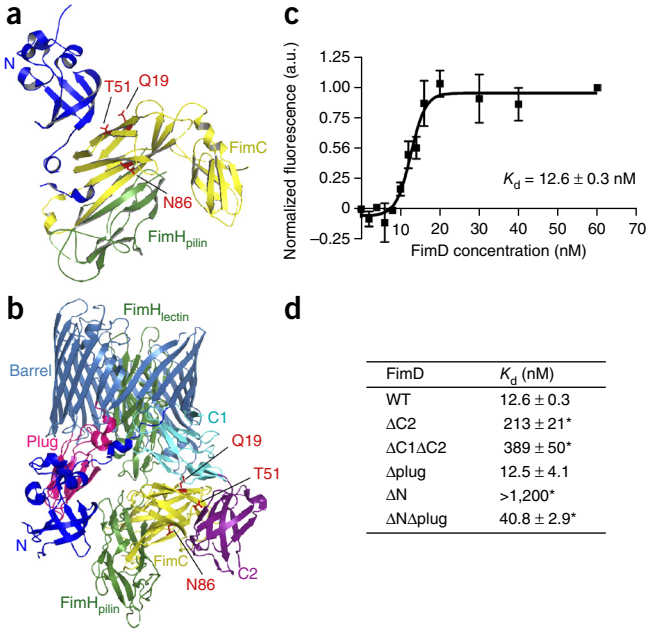

FimD	K_d (nM)
WT	12.6 ± 0.3
ΔC2	213 ± 21*
ΔC1ΔC2	389 ± 50*
Δplug	12.5 ± 4.1
ΔN	>1,200*
ΔNΔplug	40.8 ± 2.9*

Therefore, although we do not know the basis for the altered mobilities, the Tyr704 and Thr717 cross-linked products represent FimD interactions with FimH or FimC, respectively.

FimD C1 and C2 domains are the high-affinity binding site

Having validated the usher N and C domains as binding sites for chaperone–subunit complexes, we next sought to determine the relative contributions of each domain to affinity for FimC–FimH, measuring affinity (K_d) with a fluorescence-based assay[17,35]. We first measured binding affinity of WT FimD for FimC–FimH, in a system in which FimC was labeled with the thiol-reactive probe coumarin maleimide (CPM) at Q19C, T51C or N86C single-cysteine-substitution mutations. We chose these labeling sites because of their proximity to the usher when the chaperone–adhesin complex is bound at either the N or C domains[21,23] (structures shown in **Fig. 3a**,**b** and **Supplementary Fig. 4**). Each of the FimC substitution mutants expressed stably and functioned similarly to WT FimC with regard to pilus assembly in bacteria (data not shown). Binding assays with these FimC constructs yielded K_d values of 9.50–12.6 nM (**Fig. 3c** and **Supplementary Fig. 5**). The measured affinities were not significantly different ($P = 0.18$), thus indicating agreement among the different labeling sites. Moreover, these values correspond well with

Figure 3 Binding affinities of FimC–FimH chaperone–adhesin complexes for WT and domain-deleted FimD ushers. (**a**,**b**) Structures of the FimD N domain bound to a FimC–FimH pilin-domain complex (**a**) and the FimD–FimC–FimH complex (**b**). The structures and colors are as in **Figure 2**. The FimC cysteine-substitution sites Q19, T51 and N86 are shown in red in stick representation. These sites are in proximity to the usher when FimC–FimH is bound at either the N or C domains (additional structures in **Supplementary Fig. 4**). (**c**) Binding curve of FimC$_{Q19C}$–FimH for WT FimD. The graph represents normalized changes in total fluorescence emission intensity (a.u., arbitrary units) plotted as a function of FimD concentration, with a total change in intensity of 20%. The data points represent means ± s.e.m. of three independent experiments, with three replicates per experiment. (Additional data in **Supplementary Fig. 5**). (**d**) Affinities of FimC–FimH for FimD WT and domain-deletion mutants. Affinities were calculated as in **c**. (Additional binding curves of FimC–FimH for FimD WT and domain-deletion mutants are shown in **Supplementary Fig. 5**.) *$P < 0.005$ compared to WT FimD by two-tailed t test.

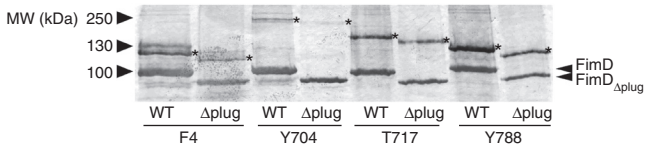

Figure 4 FimC–FimH binds to the N, C1 and C2 domains of the FimD$_{\Delta plug}$ usher *in vivo*. Anti–FimC–FimH immunoblot analysis of *in vivo* site-directed photo-cross-linking. Samples are purified histidine-tagged WT or FimD$_{\Delta plug}$ ushers containing amber mutations at positions Phe4 (N domain), Tyr704 (C1 domain), Thr717 (C1 domain) or Tyr788 (C2 domain), and associated cross-linked products. The positions of the WT and FimD$_{\Delta plug}$ monomers are indicated on the right, and the asterisks mark the cross-linked products. The uncropped image is shown in **Supplementary Data Set 2**.

a previously reported K_d of 9.1 nM determined by surface plasmon resonance[18]. We chose the FimC$_{Q19C}$ CPM-labeling site (K_d of 12.6 nM) for subsequent affinity measurements.

To examine the contribution of the usher C domains to affinity for chaperone–subunit complexes, we measured the binding to FimC–FimH of deletion mutants lacking either the C2 or both the C1 and C2 domains (FimD$_{\Delta C2}$ and FimD$_{\Delta C1\Delta C2}$, respectively). Both of these, and all other usher deletion mutants used in this study, expressed stably and folded properly in the bacterial OM (data not shown). We obtained K_d values of 213 nM and 389 nM for the FimD$_{\Delta C2}$ and FimD$_{\Delta C1\Delta C2}$ mutants, respectively (**Fig. 3d** and **Supplementary Fig. 5**). The decreased affinities obtained for these mutants compared to WT FimD identify the C domains as the high-affinity binding site on the usher for chaperone–subunit complexes. These results also reveal that the usher N domain, which remains available for binding in the FimD$_{\Delta C2}$ and FimD$_{\Delta C1\Delta C2}$ mutants (**Fig. 1b**), has lower affinity for FimC–FimH. In the P-pilus system, the isolated usher plug domain was previously shown to interact with chaperone–subunit complexes[19,36]. To determine whether the plug contributes to affinity for FimC–FimH in the context of the full-length usher, we examined a mutant lacking the plug (FimD$_{\Delta plug}$). The affinity of FimD$_{\Delta plug}$ for FimC–FimH (12.5 nM; **Fig. 3d** and **Supplementary Fig. 5**) was similar to that of WT FimD. This indicates no direct role for the plug domain, at least for binding to the initiating chaperone–adhesin complex.

The plug domain masks the C domains in the inactive usher

Given that the C domains provide the high-affinity binding site, it is not clear why the N domain is required for the initial binding of chaperone–subunit complexes to the usher. To address this question, we measured the affinity of an N domain–deletion mutant (FimD$_{\Delta N}$) for FimC–FimH. Despite the presence of the C domains, there was no appreciable binding of FimC–FimH to FimD$_{\Delta N}$ (K_d >1,200 nM; **Fig. 3d** and **Supplementary Fig. 5**). This suggests that the high-affinity C domains are unavailable for binding in the absence of the N domain. In its apo state, the usher plug domain resides within the lumen of the β-barrel channel (refs. 20,22,23 and **Supplementary Fig. 1c**). We reasoned that in this position the plug could interact with the C1 and C2 domains, thus keeping the C domains inaccessible until activation of the usher by binding of a chaperone–adhesin complex to the N domain and expulsion of the plug to the periplasm. To test this, we constructed a FimD usher lacking both the N and plug domains (FimD$_{\Delta N\Delta plug}$) (**Fig. 1b**). The affinity of FimD$_{\Delta N\Delta plug}$ for FimC–FimH was 40.8 nM (**Fig. 3d** and **Supplementary Fig. 5**), which is dramatically increased compared to the affinity of the FimD$_{\Delta N}$ mutant and close to the affinity of WT FimD. This result indicates that the high-affinity C1 and C2 domains become accessible to chaperone–subunit complexes in the absence of the plug domain, thus supporting our hypothesis that the plug functions to mask the C domains in the inactive usher.

The plug domain is required for higher-order pilus assembly

Previous studies have demonstrated that the plug domain is essential for pilus assembly by the usher[22,37,38]. Our results indicate that the plug functions to maintain the usher in the inactive state by masking the C domains, but this does not explain why the plug is necessary for pilus biogenesis. One possibility is that in the absence of the plug domain, chaperone–subunit complexes no longer bind to the N domain. We used site-directed photo-cross-linking to detect binding of FimC–FimH to the N and C domains of the FimD$_{\Delta plug}$ mutant. We obtained a similar pattern of cross-links for the FimD$_{\Delta plug}$ mutant as for WT FimD (**Fig. 4**). Notably, the level of FimD$_{\Delta plug}$ in the OM was lower than for WT FimD, and this explains the weaker appearance of the cross-linked bands for the plug-deletion mutant. Thus, chaperone–subunit complexes still interact with both the N and C domains in the absence of the plug domain.

To further investigate the role of the plug in pilus assembly, we expressed histidine-tagged WT FimD or the FimD$_{\Delta plug}$ mutant in bacteria together with the FimC chaperone and FimH and FimG pilus tip subunits. These experimental conditions allow testing of the ability of the usher to polymerize pilus fibers (consisting of FimH followed by multiple copies of FimG) with a copurification assay[39]. FimC, FimG and FimH copurified with both WT FimD and the FimD$_{\Delta plug}$ mutant, as revealed by immunoblotting with anti–FimC–FimG or anti–FimC–FimH antibodies (**Fig. 5**). Subunit-subunit, but not chaperone-subunit, interactions are stable in SDS at low temperatures[39]. Analysis of the WT FimD samples incubated at 25 °C revealed a ladder of higher-molecular-mass species, which indicated polymerization of FimG into a pilus fiber with FimH at its tip (**Fig. 5**). In contrast, examination of the FimD$_{\Delta plug}$ samples incubated at 25 °C demonstrated that the mutant was greatly impaired in its ability to promote

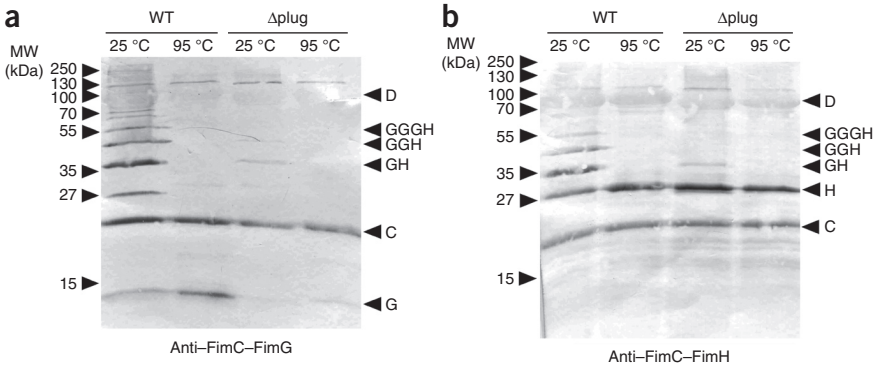

Figure 5 Assembly of type 1–pilus tip fibers by the WT and FimD$_{\Delta plug}$ ushers. (**a**,**b**) Anti–FimC–FimG (**a**) or anti–FimC–FimH (**b**) immunoblots. Samples are purified histidine-tagged WT or FimD$_{\Delta plug}$ ushers and associated pilus assembly intermediates incubated at 25 or 95 °C in SDS sample buffer. The identities of the pilus proteins and assembly intermediates are indicated on the right as single letters (C, FimC; G, FimG; H, FimH; D, FimD). Uncropped images are shown in **Supplementary Data Set 2**.

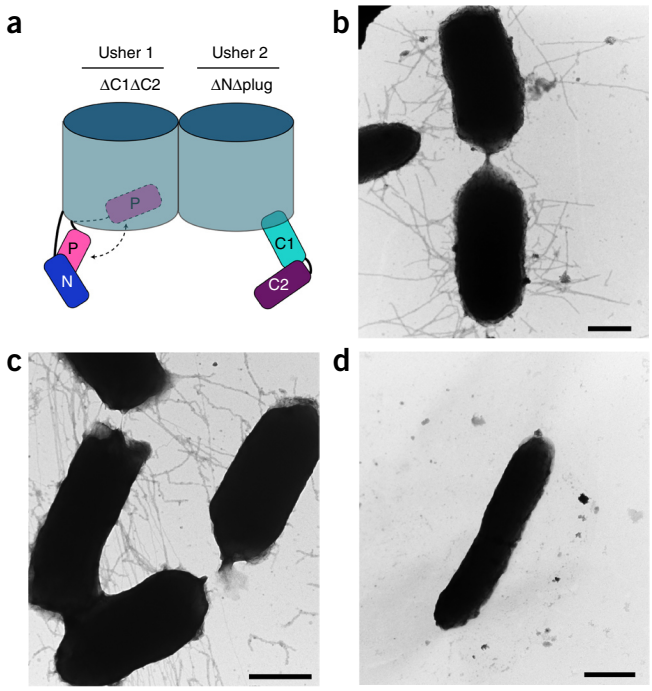

Figure 6 Coexpression of $FimD_{\Delta N\Delta plug}$ and $FimD_{\Delta C1\Delta C2}$ ushers results in pilus assembly on the bacterial surface. (**a**) Cartoon representations of the $FimD_{\Delta C1\Delta C2}$ (usher 1) and $FimD_{\Delta N\Delta plug}$ (usher 2) deletion mutants coexpressed in **c**. The N, plug (P), C1 and C2 domains present in each usher construct are indicated. (**b**–**d**) Whole-bacteria, negative-stain transmission EM of *E. coli* strain MM294Δ*fimD* expressing WT FimD (**b**), $FimD_{\Delta N\Delta plug}$ together with $FimD_{\Delta C1\Delta C2}$ (**c**) or vector only (**d**). The FimD -expression plasmids used are listed in **Table 1**. Scale bars, 500 nm.

fiber polymerization (**Fig. 5**). Concordantly, bacteria expressing the $FimD_{\Delta plug}$ mutant were unable to assemble pilus fibers of sufficient length on the bacterial surface to agglutinate red blood cells (**Supplementary Table 1**). Taking these findings together, we conclude that the plug domain is dispensable for the binding of chaperone–subunit complexes to the usher and for initiation of pilus assembly, but it is essential for efficient polymerization of the pilus fiber.

Plug deletion reveals a functional usher oligomer

The usher exists as an oligomer in the OM; however, only one usher protomer is involved in secretion of the pilus fiber, and the function of the oligomer is not known[20,23,30–32]. One possibility is that the N domains of the nontranslocating ushers recruit chaperone–subunit complexes to the OM assembly platform, and these complexes are then transferred to the C domains of the actively translocating usher. If this is true, then coexpression of $FimD_{\Delta C1\Delta C2}$ and $FimD_{\Delta N\Delta plug}$ usher mutants (with N and C domains available, respectively; **Fig. 6a**) should allow reconstitution of pilus biogenesis. Indeed, coexpression of the $FimD_{\Delta N\Delta plug}$ and $FimD_{\Delta C1\Delta C2}$ constructs resulted in assembly of functional type 1 pili, as measured by the HA assay (**Table 1**). Notably, the $FimD_{\Delta N\Delta plug}$ and $FimD_{\Delta C1\Delta C2}$ mutants did not assemble pili when expressed individually (**Table 1**). We confirmed pilus biogenesis on the bacterial surface in the strain coexpressing $FimD_{\Delta C1\Delta C2}$ and $FimD_{\Delta N\Delta plug}$ by EM, which revealed levels of pilus fibers comparable to those in the strain expressing WT FimD (**Fig. 6b–d**). Concordantly with our finding that the plug domain masks the C domains in the inactive usher, coexpression of a $FimD_{\Delta N}$ mutant (with plug domain intact) with $FimD_{\Delta C1\Delta C2}$ did not result in pilus assembly (**Table 1**). In additional experiments, we found that coexpression of $FimD_{\Delta N\Delta plug}$ with a $FimD_{\Delta plug\Delta C1\Delta C2}$ mutant did not restore pilus assembly, and neither did coexpression of $FimD_{\Delta N}$ with a $FimD_{\Delta plug\Delta C1\Delta C2}$ mutant (**Table 1**). This indicates that a plug domain must be present for successful complementation, but the plug cannot be located together with the C domains. These data demonstrate that individual usher molecules are capable of functioning in *trans* for pilus biogenesis in bacteria and provide confirmation that the plug domain masks the C domains in the inactive usher.

DISCUSSION

The usher is a remarkable molecular machine that catalyzes ordered polymerization of the pilus fiber and provides the channel for secretion of the fiber to the cell surface. The usher performs its functions in the absence of an external energy source such as ATP, relying instead on harnessing protein-protein interactions[40]. Our findings reveal mechanisms by which the usher controls access to its domains and show how these domains act in concert to ensure the assembly of adhesive organelles. We also demonstrate that individual usher molecules can act in *trans* for pilus biogenesis in bacteria, providing conclusive evidence for a functional usher oligomer.

Using site-directed photo-cross-linking, we confirmed that the usher N, C1 and C2 domains function as binding sites for chaperone–subunit complexes during pilus biogenesis in bacteria. The cross-linked products obtained for the FimD Tyr704 and Thr717 mutants, located in the C1 domain, migrated with slower-than-expected relative mobility. We did not identify other potential binding partners by mass spectrometry, and only the usher is capable of forming a cross-link in our experimental system. One possibility for the slower mobility is that these cross-linked products migrate aberrantly during electrophoresis. A second possibility is that these complexes represent higher-order assembly intermediates comprising FimD–FimD as well as FimD–FimH or FimD–FimC contacts, consistently with the usher oligomer forming an actively engaged assembly unit *in vivo*.

Our comparison of full-length and domain-deleted FimD ushers revealed that the C domains provide the high-affinity binding site for FimC–FimH chaperone–adhesin complexes. From our results, we conclude that the K_d measured for WT FimD (12.6 nM) reflects the contribution of the C domains to affinity for FimC–FimH, and the K_d measured for $FimD_{\Delta C1\Delta C2}$ (389 nM) reflects the contribution of the N domain to affinity for FimC–FimH. In contrast to our results, Volkan *et al.* found that the C2 domain of the P-pilus usher PapC had lower affinity for chaperone–subunit complexes compared to the N domain[19]. This difference probably arose because the PapC C2 domain was studied in isolation rather than in its native

Table 1 Assembly of adhesive pili on the bacterial surface by coexpression of WT or domain-deleted FimD ushers

FimD	Plasmids	HA titer[a]
WT + WT	pNH382 + pNH213	128
ΔN + ΔC1ΔC2	pNH383 + pNH295	0
ΔNΔplug + ΔC1ΔC2	pGW217 + pNH295	32
ΔNΔplug + vector	pGW217 + pMMB66	0
Vector + ΔC1ΔC2	pTRYC + pNH295	0
ΔN + ΔplugΔC1ΔC2	pNH383 + pNH423	0
ΔNΔplug + ΔplugΔC1ΔC2	pGW217 + pNH423	0

[a]HA titer is the maximum fold dilution of bacteria (strain MM294Δ*fimD* expressing the indicated FimD constructs) able to agglutinate guinea pig red blood cells.

orientation in the context of the C1 domain and the rest of the usher protein. Chaperone–subunit complexes bind first to the usher N domain and then transfer to the C domains through an unknown mechanism[21,23–25,27,28]. Our results suggest that this handoff is driven by differential affinity, with the high-affinity C domains outcompeting the lower-affinity N domain for the common binding site on the chaperone. Handoff may also be facilitated by allosteric destabilization of the N domain–chaperone–subunit complex, by the C2 domain or by interactions with the plug, as suggested by studies in the P-pilus system[19,36].

Our finding that the C domains have higher affinity than the N domain for FimC–FimH raised the question of why chaperone–subunit complexes first bind to the N domain of the apo usher. We demonstrated that the C domains are not available for binding in the absence of the N domain but become available in the absence of the plug. On the basis of these results, we propose that the apo usher uses a domain-masking strategy, which is dependent on interaction of the C domains with the plug, to keep the C domains inaccessible (**Supplementary Fig. 6**). Only FimC–FimH chaperone–adhesin complexes are able to activate the FimD usher[13,18,29]. Therefore, masking of the C domains would allow the usher to sample chaperone–subunit complexes in the periplasm via its N domain, with only FimC–FimH initiating pilus assembly by triggering release of the plug from the channel and freeing the C domains (**Supplementary Fig. 6**). Domain masking thus provides a mechanism to ensure assembly of a functional pilus fiber with the adhesin at its tip, poised to bind host-cell receptors.

The plug domain is essential for the function of the usher in pilus biogenesis[22,37,38]. The plug occupies the channel of the apo usher, and we show here that the plug masks the C domains. However, these functions are related to maintenance of the usher in its inactive state. We found that the plug domain is not needed for recruitment of chaperone–subunit complexes to the usher or for formation of stable pilus assembly intermediates *in vivo*. Instead, we found that the plug is required for efficient polymerization of the pilus fiber. The catalytic activity of the usher in fiber polymerization is postulated to be due to optimal positioning of chaperone–subunit complexes to promote the DSE reaction[23]. In the activated usher, the plug resides in the periplasm, adjacent to the N domain[23,27] (structure shown in **Supplementary Fig. 1d**). We propose that the plug contributes to catalytic activity by fixing orientation of the N domain relative to C domains. Thus, the location of the plug may act as a central switch that determines the activation state of the usher. In the resting usher, the plug closes the channel and masks the C domains. Expulsion of the plug to the periplasm then activates the usher by (i) opening the channel, (ii) unmasking the C domains and (iii) ensuring optimal positioning of the N domain to promote subunit-subunit interactions.

The usher exists as an oligomeric complex in the bacterial OM[20,23,30–32], but whether the oligomer makes a functional contribution to pilus biogenesis has been a subject of debate. We show here that coexpression of $FimD_{\Delta N\Delta plug}$ and $FimD_{\Delta C1\Delta C2}$ ushers results in assembly of adhesive pili on the bacterial surface. Pilus biogenesis by these ushers necessitates cooperative interaction between the N and C domains from different usher molecules; this provides a mechanistic basis for the function of the usher oligomer (**Supplementary Fig. 6**). Analysis of various combinations of FimD deletion mutants revealed that a plug domain is required for successful complementation, but the plug cannot be present on the same usher as the C domains. The requirement for the plug together with the N domain emphasizes the active role of the plug in the catalytic activity of the usher. The finding that complementation does not work when the plug is present together with the C domains reflects our finding that the plug masks the C domains in the inactive usher. In a prior study, we found that PapC C terminal–deletion mutants could interact with FimD to drive assembly of P pili on the bacterial surface by the Fim system[28]. This supports the existence of cooperative interactions between different ushers in bacteria. The FimH adhesin was also required for functional interaction between PapC and FimD in the prior study, thus suggesting that FimD needed to be activated by binding to the adhesin[28]. In light of the results from the current study, we can now understand that the C domains of FimD were masked and unavailable to participate in pilus assembly before usher activation.

We propose that identical usher molecules act in an asymmetric manner during pilus biogenesis, with multiple ushers serving to recruit chaperone–subunit complexes to the OM but only one usher providing the active translocation channel (**Supplementary Fig. 6**). Such an arrangement may enhance the catalytic activity of the usher by increasing the local concentration of chaperone–subunit complexes and may allow for greater regulatory control of fiber polymerization through usher-usher interactions or changes in the oligomeric state of the usher. Other transporters found in both prokaryotes and eukaryotes also exist as oligomeric complexes[41–44]. Studies have suggested that these complexes may also function in an asymmetric manner, with the oligomeric arrangement providing additional binding sites or allowing regulatory interactions[41,44–46]. Thus, the use of identical channels in an asymmetric manner may be a common strategy used by diverse transport systems.

METHODS

Methods and any associated references are available in the online version of the paper.

Note: Any Supplementary Information and Source Data files are available in the online version of the paper.

ACKNOWLEDGMENTS

We thank the Schultz laboratory (Scripps Research Institute) for providing plasmid pEVOL-pBpF. We thank S. Van Horn of the Stony Brook University Central Microscopy Imaging Center and V. Sampath (Stony Brook University) for assistance with EM. We thank J. Haley, D. Martin and R. Rieger of the Stony Brook Proteomics Center for performing the mass spectrometry analysis and for helpful discussions. We thank S. Scarlata (Stony Brook University), A.W. Karzai (Stony Brook University), K.W. Dodson (Washington University) and A.H. Delcour (University of Houston) for helpful discussions and critical reading of the manuscript. This study was supported by US National Institutes of Health (NIH) grants R01GM062987 (to D.G.T. and H.L.) and R01AI029549 (to S.J.H.). G.T.W. was supported by Medical Scientist Training Program award T32GM008444 and National Research Service Award F30AI112252 from the NIH. The Stony Brook Proteomics Center receives support from NIH award S10RR023680.

AUTHOR CONTRIBUTIONS

G.T.W., N.S.H., S.J.H., H.L. and D.G.T. designed the experiments. G.T.W., N.S.H., E.B.P. and S.S. performed the experiments. All authors were involved in data interpretation and discussion. G.T.W. and D.G.T. wrote the manuscript with contributions from all other authors.

COMPETING FINANCIAL INTERESTS

The authors declare no competing financial interests.

1. Nuccio, S.P. & Baumler, A.J. Evolution of the chaperone/usher assembly pathway: fimbrial classification goes Greek. *Microbiol. Mol. Biol. Rev.* **71**, 551–575 (2007).
2. Zav'yalov, V., Zavialov, A., Zav'yalova, G. & Korpela, T. Adhesive organelles of Gram-negative pathogens assembled with the classical chaperone/usher machinery: structure and function from a clinical standpoint. *FEMS Microbiol. Rev.* **34**, 317–378 (2010).

3. Geibel, S. & Waksman, G. The molecular dissection of the chaperone-usher pathway. *Biochim. Biophys. Acta* **1843**, 1559–1567 (2014).
4. Thanassi, D.G., Bliska, J.B. & Christie, P.J. Surface organelles assembled by secretion systems of Gram-negative bacteria: diversity in structure and function. *FEMS Microbiol. Rev.* **36**, 1046–1082 (2012).
5. Mulvey, M.A. *et al.* Induction and evasion of host defenses by type 1-piliated uropathogenic *Escherichia coli*. *Science* **282**, 1494–1497 (1998).
6. Roberts, J.A. *et al.* The Gal(alpha1–4)Gal-specific tip adhesin of *Escherichia coli* P-fimbriae is needed for pyelonephritis to occur in the normal urinary tract. *Proc. Natl. Acad. Sci. USA* **91**, 11889–11893 (1994).
7. Jones, C.H. *et al.* FimH adhesin of type-1 pili is assembled into a fibrillar tip structure in the *Enterobacteriaceae*. *Proc. Natl. Acad. Sci. USA* **92**, 2081–2085 (1995).
8. Hahn, E. *et al.* Exploring the 3D molecular architecture of *Escherichia coli* type 1 pili. *J. Mol. Biol.* **323**, 845–857 (2002).
9. Lycklama a Nijeholt, J.A. & Driessen, A.J. The bacterial Sec-translocase: structure and mechanism. *Phil. Trans. R. Soc. Lond. B* **367**, 1016–1028 (2012).
10. Choudhury, D. *et al.* X-ray structure of the FimC-FimH chaperone-adhesin complex from uropathogenic *Escherichia coli*. *Science* **285**, 1061–1066 (1999).
11. Sauer, F.G. *et al.* Structural basis of chaperone function and pilus biogenesis. *Science* **285**, 1058–1061 (1999).
12. Zavialov, A.V. *et al.* Structure and biogenesis of the capsular F1 antigen from *Yersinia pestis*: preserved folding energy drives fiber formation. *Cell* **113**, 587–596 (2003).
13. Nishiyama, M., Ishikawa, T., Rechsteiner, H. & Glockshuber, R. Reconstitution of pilus assembly reveals a bacterial outer membrane catalyst. *Science* **320**, 376–379 (2008).
14. Sauer, F.G., Pinkner, J.S., Waksman, G. & Hultgren, S.J. Chaperone priming of pilus subunits facilitates a topological transition that drives fiber formation. *Cell* **111**, 543–551 (2002).
15. Rose, R.J. *et al.* Unraveling the molecular basis of subunit specificity in P pilus assembly by mass spectrometry. *Proc. Natl. Acad. Sci. USA* **105**, 12873–12878 (2008).
16. Nishiyama, M. & Glockshuber, R. The outer membrane usher guarantees the formation of functional pili by selectively catalyzing donor-strand exchange between subunits that are adjacent in the mature pilus. *J. Mol. Biol.* **396**, 1–8 (2010).
17. Li, Q. *et al.* The differential affinity of the usher for chaperone-subunit complexes is required for assembly of complete pili. *Mol. Microbiol.* **76**, 159–172 (2010).
18. Saulino, E.T., Thanassi, D.G., Pinkner, J.S. & Hultgren, S.J. Ramifications of kinetic partitioning on usher-mediated pilus biogenesis. *EMBO J.* **17**, 2177–2185 (1998).
19. Volkan, E. *et al.* Domain activities of PapC usher reveal the mechanism of action of an *Escherichia coli* molecular machine. *Proc. Natl. Acad. Sci. USA* **109**, 9563–9568 (2012).
20. Remaut, H. *et al.* Fiber formation across the bacterial outer membrane by the chaperone/usher pathway. *Cell* **133**, 640–652 (2008).
21. Nishiyama, M. *et al.* Structural basis of chaperone-subunit complex recognition by the type 1 pilus assembly platform FimD. *EMBO J.* **24**, 2075–2086 (2005).
22. Huang, Y., Smith, B.S., Chen, L.X., Baxter, R.H. & Deisenhofer, J. Insights into pilus assembly and secretion from the structure and functional characterization of usher PapC. *Proc. Natl. Acad. Sci. USA* **106**, 7403–7407 (2009).
23. Phan, G. *et al.* Crystal structure of the FimD usher bound to its cognate FimC–FimH substrate. *Nature* **474**, 49–53 (2011).
24. Ng, T.W., Akman, L., Osisami, M. & Thanassi, D.G. The usher N terminus is the initial targeting site for chaperone-subunit complexes and participates in subsequent pilus biogenesis events. *J. Bacteriol.* **186**, 5321–5331 (2004).
25. Dubnovitsky, A.P. *et al.* Conserved hydrophobic clusters on the surface of the Caf1A usher C-terminal domain are important for F1 antigen assembly. *J. Mol. Biol.* **403**, 243–259 (2010).
26. Eidam, O., Dworkowski, F.S., Glockshuber, R., Grutter, M.G. & Capitani, G. Crystal structure of the ternary FimC-FimF(t)-FimD(N) complex indicates conserved pilus chaperone-subunit complex recognition by the usher FimD. *FEBS Lett.* **582**, 651–655 (2008).
27. Geibel, S., Procko, E., Hultgren, S.J., Baker, D. & Waksman, G. Structural and energetic basis of folded-protein transport by the FimD usher. *Nature* **496**, 243–246 (2013).
28. So, S.S. & Thanassi, D.G. Analysis of the requirements for pilus biogenesis at the outer membrane usher and the function of the usher C-terminus. *Mol. Microbiol.* **60**, 364–375 (2006).
29. Munera, D., Hultgren, S. & Fernandez, L.A. Recognition of the N-terminal lectin domain of FimH adhesin by the usher FimD is required for type 1 pilus biogenesis. *Mol. Microbiol.* **64**, 333–346 (2007).
30. Thanassi, D.G. *et al.* The PapC usher forms an oligomeric channel: implications for pilus biogenesis across the outer membrane. *Proc. Natl. Acad. Sci. USA* **95**, 3146–3151 (1998).
31. Li, H. *et al.* The outer membrane usher forms a twin-pore secretion complex. *J. Mol. Biol.* **344**, 1397–1407 (2004).
32. Allen, W.J., Phan, G., Hultgren, S.J. & Waksman, G. Dissection of pilus tip assembly by the FimD usher monomer. *J. Mol. Biol.* **425**, 958–967 (2013).
33. Young, T.S., Ahmad, I., Yin, J.A. & Schultz, P.G. An enhanced system for unnatural amino acid mutagenesis in *E. coli*. *J. Mol. Biol.* **395**, 361–374 (2010).
34. Chin, J.W., Martin, A.B., King, D.S., Wang, L. & Schultz, P.G. Addition of a photocrosslinking amino acid to the genetic code of *Escherichia coli*. *Proc. Natl. Acad. Sci. USA* **99**, 11020–11024 (2002).
35. Royer, C.A. & Scarlata, S.F. Fluorescence approaches to quantifying biomolecular interactions. *Methods Enzymol.* **450**, 79–106 (2008).
36. Morrissey, B. *et al.* The role of chaperone-subunit usher domain interactions in the mechanism of bacterial pilus biogenesis revealed by ESI-MS. *Mol. Cell. Proteomics* **11**, M111.015289 (2012).
37. Mapingire, O.S., Henderson, N.S., Duret, G., Thanassi, D.G. & Delcour, A.H. Modulating effects of the plug, helix and N- and C-terminal domains on channel properties of the PapC usher. *J. Biol. Chem.* **284**, 36324–36333 (2009).
38. Yu, X. *et al.* Caf1A usher possesses a Caf1 subunit-like domain that is crucial for Caf1 fibre secretion. *Biochem. J.* **418**, 541–551 (2009).
39. Henderson, N.S., Ng, T.W., Talukder, I. & Thanassi, D.G. Function of the usher N-terminus in catalysing pilus assembly. *Mol. Microbiol.* **79**, 954–967 (2011).
40. Thanassi, D.G., Stathopoulos, C., Karkal, A. & Li, H. Protein secretion in the absence of ATP: the autotransporter, two-partner secretion, and chaperone/usher pathways of Gram-negative bacteria. *Mol. Membr. Biol.* **22**, 63–72 (2005).
41. Deville, K. *et al.* The oligomeric state and arrangement of the active bacterial translocon. *J. Biol. Chem.* **286**, 4659–4669 (2011).
42. Rehling, P. *et al.* Protein insertion into the mitochondrial inner membrane by a twin-pore translocase. *Science* **299**, 1747–1751 (2003).
43. Ahting, U. *et al.* Tom40, the pore-forming component of the protein-conducting TOM channel in the outer membrane of mitochondria. *J. Cell Biol.* **153**, 1151–1160 (2001).
44. Reichow, S.L. *et al.* Allosteric mechanism of water-channel gating by Ca^{2+}–calmodulin. *Nat. Struct. Mol. Biol.* **20**, 1085–1092 (2013).
45. Dalal, K., Chan, C.S., Sligar, S.G. & Duong, F. Two copies of the SecY channel and acidic lipids are necessary to activate the SecA translocation ATPase. *Proc. Natl. Acad. Sci. USA* **109**, 4104–4109 (2012).
46. Mao, C. *et al.* Stoichiometry of SecYEG in the active translocase of *Escherichia coli* varies with precursor species. *Proc. Natl. Acad. Sci. USA* **110**, 11815–11820 (2013).

ONLINE METHODS

Strains and plasmids. The bacterial strains and plasmids used in this study are listed in **Supplementary Table 2**. Unless otherwise noted, bacteria were grown at 37 °C with aeration in LB medium. When appropriate, the growth medium was supplemented with antibiotics as follows: 100 μg/ml ampicillin (Amp); 50 μg/ml kanamycin (Kan); 100 μg/ml spectinomycin (Spec); 25 μg/ml chloramphenicol (Clm); and 15 μg/ml tetracycline (Tet).

The molecular-biology techniques and primers used to construct the plasmids made in this study are listed in **Supplementary Table 3**. *E. coli* DH5α was used as the host strain for plasmid manipulations. The FimD amber mutants used for site-directed photo-cross-linking were derived from plasmids pNH213 or pNH400 with QuikChange site-directed mutagenesis (Stratagene). Plasmid pNH213 encodes the FimD usher with a C-terminal, thrombin-cleavable polyhistidine tag (His tag) under isopropyl-β-D-thiogalactoside (IPTG)-inducible expression. For pNH400, the His tag of plasmid pNH213 was switched to a streptavidin (strep) tag with site-directed, ligase-independent mutagenesis (SLIM)[47,48]. The FimC cysteine mutants for fluorescence labeling were derived from pETS1000 with QuikChange mutagenesis. Plasmid pETS1000 encodes the FimC chaperone with a C-terminal His tag under arabinose-inducible expression. Plasmid pNH324, encoding $FimD_{\Delta plug}$, was derived from pNH213 with SLIM to delete residues 244–323. In addition to deletion of the plug domain, an N243G substitution mutation was created. Similarly, the plug domain was deleted from plasmids pNH295 and pNH296, encoding $FimD_{\Delta C1\Delta C2}$ and $FimD_{\Delta N}$, respectively, to make plasmids pNH423 and pGW117. All constructs generated with SLIM or QuikChange mutagenesis methods were sequenced to verify that the correct mutations were made.

***In vivo* site-directed photo-cross-linking.** Strain SF100 was transformed with plasmid pEVOL-pBpF, encoding an arabinose-inducible amber suppressor tRNA and aminoacyl-tRNA synthetase, to allow incorporation of pBpa at amber stop codons (TAG)[33]. Strain SF100/pEVOL-pBpF was then transformed with plasmid pNH212, encoding IPTG-inducible FimC and FimH proteins. Finally, strain SF100/pEVOL-pBpF + pNH212 was transformed with plasmids for IPTG-inducible expression of His-tagged WT FimD (pNH213) or FimD Phe4 (pNH319), Tyr704 (pNH320), Thr717 (pNH321), or Tyr788 (pNH329) amber-codon mutants. Overnight cultures were diluted 1:20 into 30–50 ml fresh LB containing 0.2 mM *p*Bpa (VWR). Cultures were induced at an OD_{600} of 0.6 with 0.1% arabinose and 50 μM IPTG for 1–2 h. Cultures were pelleted and resuspended in 1 ml 20 mM Tris-HCl, pH 8.0, transferred to wells in an untreated six-well culture plate (CytoOne), and exposed to a UV lamp (365 nm, 100 W, Fisher Scientific) for 10 min. Exposed bacteria were then transferred to microcentrifuge tubes and pelleted at maximum speed in a microcentrifuge for 15 min at 4 °C. Pellets were weighed and resuspended in 500 μl BugBuster Master Mix (Novagen) per 0.1 g wet weight. EDTA-free cOmplete protease inhibitor (Roche) was added, and the samples were rocked for 20 min at room temperature. Samples were then spun at maximum speed in a microcentrifuge for 20 min at 4 °C, and supernatant fractions were transferred to clean tubes. Imidazole was added to 20 mM, 50 μl of 50% Ni-NTA agarose beads (Qiagen) was then added and samples were rocked for 30 min at room temperature. The beads were washed three times with 1 ml 20 mM Tris-HCl, pH 8.0, 0.3 M NaCl and 20 mM imidazole, and then boiled in 60 μl of 2× SDS-PAGE sample buffer. Boiled samples were separated by SDS-PAGE and analyzed either by staining with Coomassie blue or immunoblotting with anti–His tag (BioLegend, cat. no. MMS-156P; validation profile provided on manufacturer's website), anti–FimC–FimH[20] or anti–FimC–FimG[20] antibodies. The blots were developed with alkaline phosphatase–conjugated secondary anti-mouse (Sigma cat. no. A9316) or anti-rabbit (Sigma cat. no. A3812) antibodies and BCIP (5-bromo-4-chloro-3-indolylphosphate)-NBT (nitroblue tetrazolium) substrate (KPL).

For some experiments, SF100/pEVOL-pBpF + pNH212 strains expressing strep-tagged instead of His-tagged FimD were used (plasmids pNH400 through pNH404). For these experiments, after UV exposure, OM fractions were isolated as previously described[24]. The OM fractions were separated by SDS-PAGE and analyzed by immunoblotting with anti–His tag or anti–FimC–FimH antibodies, as described above. The expression and folding of the FimD amber mutants in the OM was compared with WT FimD, as described below. SF100/pEVOL-pBpF was used as the host strain for these experiments, and the bacteria were grown in the presence of 0.2 mM *p*Bpa. The ability of the FimD amber mutants to assemble adhesive pili on the bacterial surface was compared with that of WT FimD with the HA assay, as described below. For these assays, MM294Δ*fimD*/pEVOL-pBpF was used as the host strain, and the bacteria were grown in the presence of 0.2 mM *p*Bpa.

Mass spectrometry analysis of cross-linked products. Excised gel pieces were destained, reduced, alkylated and digested with trypsin (Promega Gold, mass-spectrometry grade), essentially as previously described[49]. The resulting concentrated peptide extract was diluted into a solution of 2% acetonitrile (ACN) and 0.1% formic acid (FA) (buffer A) for analysis. The peptide mixture was analyzed by automated microcapillary liquid chromatography–tandem mass spectrometry. Fused-silica capillaries (100 μm i.d.) were pulled with a P-2000 CO_2 laser puller (Sutter Instruments) to a tip with i.d. <5 μm and packed with 10 cm of 5 μm ProntoSil 120-5-C18H material (Agilent) with a pressure bomb. The column was installed inline with an Eksigent Nano2D High Performance Liquid Chromatography (HPLC) pump running at 300 nl min^{-1}. The column was equilibrated in buffer A, and the peptide mixture was loaded onto the column with an autosampler. The HPLC separation was provided by a gradient between buffer A and buffer B (98% ACN and 0.1% FA). The HPLC gradient was held constant at 100% buffer A for 10 min after peptide loading, and this was followed by a 35-min gradient from 0% buffer B (100% buffer A) to 40% buffer B. Then another gradient was performed for 3 min to 80% buffer B, at which point it was held constant for 2 min. Finally, the gradient was changed from 80% buffer B to 100% buffer A over 1 min and then held constant at 100% buffer A for 29 more minutes. The application of a 1.8-kV distal voltage electrosprayed the eluted peptides directly into a Thermo Fisher Scientific LTQ XL ion-trap mass spectrometer equipped with a custom-built nanoLC electrospray ionization source. Full mass spectra (MS) were recorded on the peptides over a 400–2,000 m/z range; this was followed by five tandem mass (MS/MS) events sequentially generated in a data-dependent manner on the first, second, third, fourth and fifth most intense ions selected from the full MS spectrum (at 35% collision energy). Mass spectrometer scan functions and HPLC solvent gradients were controlled by the Xcalibur data system (ThermoFinnigan). The resultant MS/MS spectra were extracted from the RAW file with Readw.exe (http://sourceforge.net/projects/sashimi/). The resulting mzXML file contains all the data for all MS/MS spectra and can be read by the subsequent analysis software. The MS/MS data were searched with InsPecT[50] and GPM X!Tandem against the Ecoli_K12 UniProt database (downloaded 3/19/2013) with optional modifications: +16 on methionine, +57 on cysteine, and +80 on threonine, serine and tyrosine. Only peptides with a P value ≤0.01 were analyzed further. Common contaminants (for example, keratins) were removed from the database. Proteins identified by at least two distinct peptides within a sample were considered valid.

Purification of FimD and FimC–FimH for affinity measurements. The WT FimD usher and FimD domain-deletion mutants contained C-terminal, thrombin-cleavable His tags and were purified as previously described[51]. Briefly, 6-l cultures of strain Tuner containing plasmid pNH213 (WT FimD), pNH295 ($FimD_{\Delta C1\Delta C2}$), pNH317 ($FimD_{\Delta C2}$), pNH296 ($FimD_{\Delta N}$), pNH324 ($FimD_{\Delta plug}$) or pGW117 ($FimD_{\Delta N\Delta plug}$) were induced for usher expression at an OD_{600} of 0.6 with 100 μM IPTG and grown overnight at room temperature. Bacteria were lysed with a French press, and the OM fraction was isolated by sarkosyl extraction and centrifugation. OM fractions were then solubilized in 20 mM Tris-HCl, pH 8, 0.3 M NaCl and 1% dodecyl-maltopyranoside (DDM; Anatrace). Imidazole was added to 20 mM, and the samples were loaded onto a cobalt affinity column with an FPLC apparatus (GE Healthcare). The bound FimD protein was eluted with an imidazole step gradient in buffer 20 mM Tris-HCl, pH 8, 0.3 M NaCl and 10 mM lauryl(dimethyl)amine oxide (LDAO; Anatrace). The His tag was cleaved by digestion with thrombin overnight, and then the sample was passed again over a cobalt affinity column coupled to a benzamidine column (GE Healthcare). The pure, His tag–free FimD was collected in the flow-through fraction. The purified usher was dialyzed into 20 mM HEPES, pH 7.5, 150 mM NaCl and 5 mM LDAO, and concentrated with a Millipore Ultrafree centrifugal concentrator (50-kDa molecular-weight cutoff). Protein concentrations were determined with the bicinchoninic acid (BCA) protein assay (Pierce).

FimC–FimH complexes were purified from strain Tuner/pHJ20 containing plasmid pGW1 ($FimC_{T51C}$), pGW2 ($FimC_{N86C}$) or pGW3 ($FimC_{Q19C}$). Plasmid pHJ20 encodes IPTG-inducible FimH, and plasmids pGW1–3 encode

doi:10.1038/nsmb.3044

arabinose-inducible, His-tagged FimC with the indicated cysteine substitutions. Purification was performed as previously described[51]. Briefly, 2-l cultures were grown at 37 °C and induced at an OD_{600} of 0.6 with 0.002% arabinose and 1 mM IPTG for 2 h. Periplasm fractions were isolated by EDTA-lysozyme treatment and dialyzed into 20 mM Tris-HCl, pH 8.0, and 0.3 M NaCl. Imidazole was added to 20 mM, and samples were loaded onto a nickel affinity column with an FPLC apparatus. Bound FimC–FimH complex was eluted with an imidazole step gradient. Fractions containing FimC–FimH were pooled and dialyzed into 20 mM MES, pH 5.4. The samples were then run on a Resource S column (GE Healthcare) and eluted with a linear NaCl gradient to separate excess unbound FimC chaperone from the FimC–FimH chaperone–adhesin complex.

Fluorescence-based affinity assay. Fluorescence-labeling reactions and titration experiments were performed as previously described[17,35]. $FimC_{Q19C}$–, $FimC_{T51C}$– and $FimC_{N86C}$–FimH complexes (500 nM) were labeled with the thiol-reactive probe coumarin maleimide (Life Technologies) for 2 h at 4 °C at a 5:1 probe/protein molar ratio. For labeling, the pH of the protein solution was first raised to 8.0 via the addition of K_2HPO_4. Unbound probe was removed via dialysis against 20 mM HEPES, pH 7.5, and 150 mM NaCl. 5 mM LDAO was added to the final exchanged solution. Labeling efficiency was calculated with Beer's Law and was typically >80%.

Fluorescence measurements were performed with a PC1 photon-counting spectrofluorometer (ISS), as previously described[17]. Coumarin-labeled chaperone–subunit complexes were diluted to 25 nM, and 120 µl was transferred to a 3-mm microcuvette. Purified FimD was then titrated into the FimC–FimH solution. The fluorophore was excited at 384 nM, and its emission spectrum was measured from 420–520 nm with a step size of 2 nm. Variability in lamp intensity was accounted for with Vinci (ISS) data-acquisition software. The integral of the curve was calculated, thus providing the total emission intensity. Buffer measurements were also performed, and background emissions were subtracted. Data were normalized to account for dilution during titration and were set to a scale of 0 (starting value) to 1 (the final value). Apparent equilibrium bimolecular dissociation constants (K_d) were obtained by fitting the data with a sigmoidal curve function in Prism (GraphPad) and solving for the inflection point. Each titration curve shown is the result of at least three independent experiments with three replicates per experiment. All of our observed K_d values were independent of starting FimC–FimH concentrations (below the dissociation constant) and thus were dependent only on the mass action of the titrant, FimD. Statistical comparison of K_d values for FimD mutants with WT FimD was performed with two-tailed *t* tests in Prism (GraphPad). Comparison of the different FimC cysteine-substitution mutants was performed with one-way analysis of variance and Tukey's multiple-comparison post test. *P* values <0.05 were considered significant.

Analysis of usher expression and folding in the OM. The expression levels and folding of the FimD mutants in the OM were compared to WT FimD, as previously described[39]. Briefly, OM fractions were isolated by French-press disruption and sarkosyl extraction, and proper folding of the ushers was determined by heat-modifiable mobility on SDS-PAGE. Strain SF100 was used as the host strain for these studies.

Hemagglutination (HA) assay. HA assays were performed by serial dilution in microtiter plates, as previously described[39]. HA titers were determined visually and are reported as the greatest fold dilution of bacteria able to agglutinate guinea pig red blood cells (Colorado Serum Company). For each HA assay, at least three independent experiments were performed, with three replicates per experiment. Analysis of the FimC WT and cysteine-substitution mutants was performed in strain MM294Δ*fimC*, which contains a *fimC* deletion in the chromosomal *fim* operon. Analysis of the FimD WT and mutant ushers was performed in strain MM294Δ*fimD*, which contains a *fimD* deletion in the chromosomal *fim* operon. The experiments in which FimD WT or domain deletion–mutant ushers were coexpressed were also performed in strain MM294Δ*fimD*. Bacteria containing appropriate FimD or FimC plasmids were grown statically for 24–48 h to induce the chromosomal *fim* genes, and then FimD or FimC expression was induced with 50 µM IPTG or 0.15% arabinose, respectively, for an additional 3 h with shaking at 100 r.p.m. To test the role of OmpA in type 1–pilus biogenesis, HA titers were determined for strain JF568 and its isogenic *ompA*$^-$ derivative JF699. The strains were grown statically for 24–48 h to induce the chromosomal *fim* genes. For analysis of assembly of FimG–FimH type 1–pilus tips, strain AAEC185/pNH222 (encoding FimC, FimG and FimH) was transformed with the FimD-expression plasmids pNH213 (WT FimD) or pNH324 ($FimD_{\Delta plug}$). HA titers were determined from strains grown with aeration and induced at an OD_{600} of 0.6 with 50 µM IPTG and 0.1% arabinose for 1 h.

Electron microscopy (EM). Whole-bacteria negative-stain transmission EM was performed as previously described[24]. Aliquots (1 ml) of cultures grown for the HA assay were washed with PBS and resuspended in 1.5 ml PBS. Bacteria were fixed with 1% glutaraldehyde in PBS, washed with PBS followed by water and then stained for 20 s with phosphotungstic acid. Grids were examined on a TECNAI 12 BioTwin G02 microscope (FEI), and representative images were acquired with an XR-60 CCD digital camera system (Advanced Microscopy Techniques).

Copurification of type 1–pilus assembly intermediates with WT and $FimD_{\Delta plug}$ ushers. Copurification assays were performed as previously described[39]. Briefly, OM fractions were isolated by French-press disruption and sarkosyl extraction from strain AAEC185/pNH222 containing plasmids pNH213 or pNH324, grown as described for the HA assay. OM fractions were solubilized with the nondenaturing detergent DDM, and the His-tagged FimD was purified by cobalt affinity chromatography. FimD-containing fractions from the column were incubated for 10 min at 25 or 95 °C in SDS-PAGE sample buffer, separated by SDS-PAGE, and immunoblotted with anti–FimC–FimH[20] or anti–FimC–FimG[20] antibodies to detect pilus assembly intermediates that copurified with the usher. Immunoblots were developed with alkaline phosphatase–conjugated secondary anti-rabbit (Sigma cat. no. A3812) antibody and BCIP-NBT substrate (KPL). Original images of gels and blots used in this study can be found in **Supplementary Data Set 2**.

47. Chiu, J., March, P.E., Lee, R. & Tillett, D. Site-directed, Ligase-Independent Mutagenesis (SLIM): a single-tube methodology approaching 100% efficiency in 4 h. *Nucleic Acids Res.* **32**, e174 (2004).
48. Chiu, J., Tillett, D., Dawes, I.W. & March, P.E. Site-directed, Ligase-Independent Mutagenesis (SLIM) for highly efficient mutagenesis of plasmids greater than 8kb. *J. Microbiol. Methods* **73**, 195–198 (2008).
49. Shevchenko, A., Wilm, M., Vorm, O. & Mann, M. Mass spectrometric sequencing of proteins silver-stained polyacrylamide gels. *Anal. Chem.* **68**, 850–858 (1996).
50. Tanner, S. *et al.* InsPecT: identification of posttranslationally modified peptides from tandem mass spectra. *Anal. Chem.* **77**, 4626–4639 (2005).
51. Henderson, N.S. & Thanassi, D.G. Purification of the outer membrane usher protein and periplasmic chaperone-subunit complexes from the P and type 1 pilus systems. *Methods Mol. Biol.* **966**, 37–52 (2013).